

## Strain-Induced Exciton Hybridization in WS<sub>2</sub> Monolayers Unveiled by Zeeman-Splitting Measurements

Elena Blundo<sup>1,\*</sup>, Paulo E. Faria Junior<sup>2,†</sup>, Alessandro Surrente<sup>1,3</sup>, Giorgio Pettinari<sup>1,4</sup>, Mikhail A. Prosnikov<sup>5</sup>, Katarzyna Olkowska-Pucko<sup>6</sup>, Klaus Zollner<sup>2</sup>, Tomasz Woźniak<sup>7</sup>, Andrey Chaves<sup>8,9</sup>, Tomasz Kazimierczuk<sup>6</sup>, Marco Felici<sup>1</sup>, Adam Babiński<sup>6</sup>, Maciej R. Molas<sup>6</sup>, Peter C. M. Christianen<sup>5</sup>, Jaroslav Fabian<sup>2</sup>, and Antonio Polimeni<sup>1,‡</sup>

<sup>1</sup>Physics Department, Sapienza University of Rome, 00185 Rome, Italy  
<sup>2</sup>Institute for Theoretical Physics, University of Regensburg, 93040 Regensburg, Germany  
<sup>3</sup>Department of Experimental Physics, Faculty of Fundamental Problems of Technology, Wrocław University of Science and Technology, 50-370 Wrocław, Poland  
<sup>4</sup>Institute for Photonics and Nanotechnologies, National Research Council, 00156 Rome, Italy  
<sup>5</sup>High Field Magnet Laboratory, HFML-EMFL, Radboud University, 6525 ED Nijmegen, The Netherlands  
<sup>6</sup>Institute of Experimental Physics, Faculty of Physics, University of Warsaw, Pasteura 5, 02-093 Warsaw, Poland  
<sup>7</sup>Department of Semiconductor Materials Engineering, Wrocław University of Science and Technology, 50-370 Wrocław, Poland  
<sup>8</sup>Departamento de Física, Universidade Federal do Ceará, 60455-900 Fortaleza, Ceará, Brazil  
<sup>9</sup>Department of Physics, University of Antwerp, Groenenborgerlaan 171, B-2020 Antwerpen, Belgium

 (Received 22 December 2021; accepted 9 June 2022; published 4 August 2022)

Mechanical deformations and ensuing strain are routinely exploited to tune the band gap energy and to enhance the functionalities of two-dimensional crystals. In this Letter, we show that strain leads also to a strong modification of the exciton magnetic moment in WS<sub>2</sub> monolayers. Zeeman-splitting measurements under magnetic fields up to 28.5 T were performed on single, one-layer-thick WS<sub>2</sub> microbubbles. The strain of the bubbles causes a hybridization of  $k$ -space direct and indirect excitons resulting in a sizable decrease in the modulus of the  $g$  factor of the ground-state exciton. These findings indicate that strain may have major effects on the way the valley number of excitons can be used to process binary information in two-dimensional crystals.

DOI: [10.1103/PhysRevLett.129.067402](https://doi.org/10.1103/PhysRevLett.129.067402)

**Introduction.**—Transition metal dichalcogenides (TMD) monolayers (MLs) are two-dimensional (2D) crystals whose symmetry-related electronic and optical properties provide a wealth of opportunities [1,2]. For instance, the valley quantum number—associated with the  $\pm K$  band edges at the corners of the hexagonal Brillouin zone—can be used to encode and process binary information via exciton-mediated absorption and emission of circularly polarized light of opposite helicity [3]. Indeed, excitons in TMD MLs can be regarded as valley-carrying bits, whose characteristics are embodied in the gyromagnetic ( $g$ ) factor determinable by magneto-optical spectroscopies [4–20]. Under magnetic field, excitons involving the  $\pm K$  states (with  $\sigma^\pm$  polarization) separate in energy ( $E$ ) resulting in a Zeeman splitting (ZS):

$$ZS(B) = E^{\sigma^+} - E^{\sigma^-} = g_{\text{exc}} \cdot \mu_B B = 2(g_c - g_v) \cdot \mu_B B, \quad (1)$$

where  $\mu_B$  is the Bohr magneton,  $g_{\text{exc}}$  is the exciton  $g$  factor, and  $g_c$  and  $g_v$  are the conduction band (CB) and valence band (VB)  $g$  factors.

Many reports addressed the  $g$  factor of excitons in TMD MLs [4–22] and heterostructures [23–28] but the influence of strain has not been systematically studied. Strain is a fundamental tool in semiconductor research and industry to modify the electronic, optical, and transport properties of the materials and to improve device performances [29–32]. Strain is especially important for 2D crystals, which are extremely flexible and where strain is often unavoidably present. While strain effects in 2D materials have been widely studied in the past decade [33,34], the interplay between strain and exciton magnetic moment has not been investigated. In fact, typical straining devices [33,34] hardly fit within a bore magnet, and performing highly resolved experiments on microscale regions under high magnetic fields is challenging.

In this Letter, we present unprecedented ZS measurements on WS<sub>2</sub> MLs under high tensile strain (biaxial strain  $\epsilon_{\text{biax}}$  up to  $\sim 2\%$ ) and intense magnetic fields (up to 28.5 T). The mechanical deformation is attained by creating hydrogen-filled, one-layer-thick WS<sub>2</sub> microbubbles [35,36], which are studied by microphotoluminescence ( $\mu$ -PL)

Published by the American Physical Society under the terms of the [Creative Commons Attribution 4.0 International license](https://creativecommons.org/licenses/by/4.0/). Further distribution of this work must maintain attribution to the author(s) and the published article's title, journal citation, and DOI.

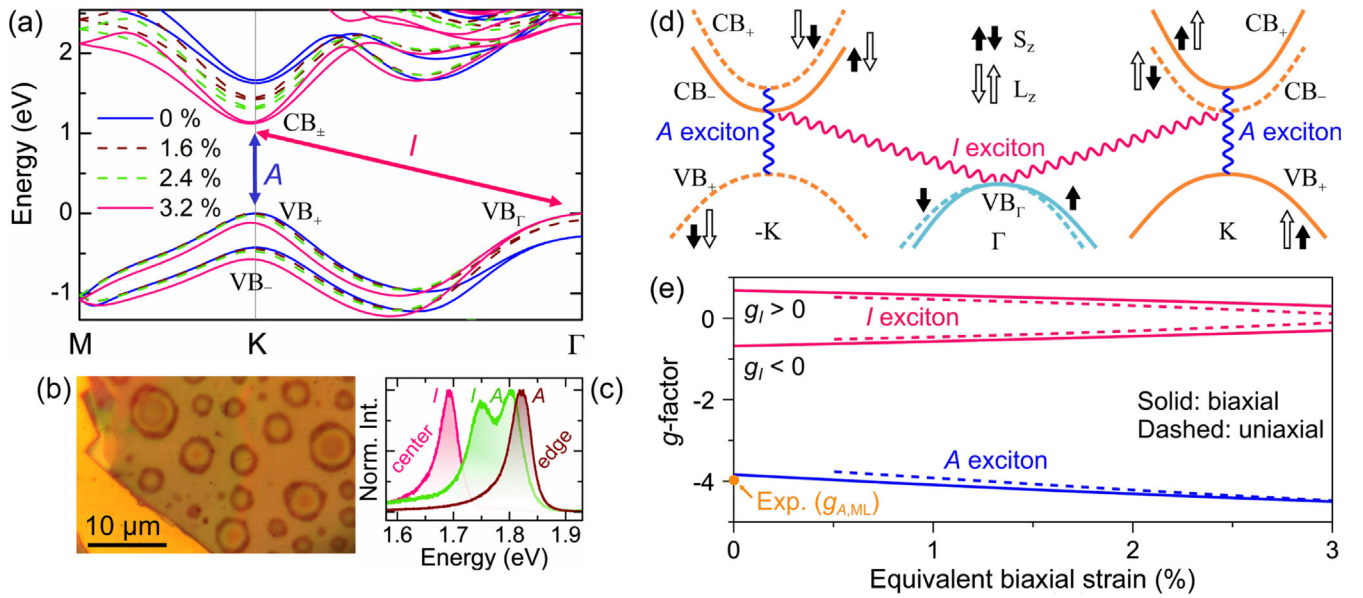


FIG. 1. (a) First-principles calculations of the band structure of WS<sub>2</sub> ML for different biaxial tensile strain values (see Supplemental Material [41], Note II). (b) Optical micrograph showing one-layer-thick WS<sub>2</sub> bubbles formed by H-ion irradiation. (c) PL spectra acquired along the radius of a WS<sub>2</sub> bubble (at its edge, center, and in between), showing a direct-to-indirect transition. (d) Schematic of the important bands that constitute the A (CB<sub>+</sub>, VB<sub>+</sub>) and I (CB<sub>-</sub>, VB<sub>Γ</sub>) transitions. The arrows indicate the orientations of L<sub>z</sub>, and S<sub>z</sub>. (e) First-principles calculations for the A and I exciton *g* factors under biaxial (solid lines) and uniaxial (dashed lines) strain. The *g* factors are plotted as a function of the equivalent biaxial strain (average of the two perpendicular strain components). The experimental *g* factor at null strain is shown for comparison.

measurements. The strain-induced crossover in the VB maximum from *K* to  $\Gamma$  permits us to select the light emission from direct (A, involving the *K* point in both CB and VB) or indirect (I, involving *K* in CB and  $\Gamma$  in VB) excitons [37]. For the A exciton in a strain-free WS<sub>2</sub> ML, we find  $g_A = -3.913$ , while values between  $-2$  and  $-3$  are measured for A and I excitons for  $\varepsilon_{\text{biax}} \sim 2\%$ . Based on first-principles calculations and phenomenological modeling, we ascribe these sizable strain-dependent variations of  $g_{\text{exc}}$  to a hybridization of A and I excitons occurring when strain brings them into near-resonance conditions. Our evidences of exciton hybridization in a 2D system open the doors to novel research in the field, where, e.g., exciton hybridization could influence the pair lifetime and efficiency or could represent an important ingredient in understanding the coupling between different materials in 2D heterostructures.

*Experimental details.*—We investigated strained WS<sub>2</sub> MLs in the shape of microbubbles [35,36]. The bubbles were created by hydrogen-ion irradiation of bulk WS<sub>2</sub> flakes, as reported in Ref. [35]. One-layer-thick bubbles with diameters up to several microns and a height-to-radius ratio of  $\sim 0.16$  swell from the flake due to the trapping of hydrogen at tens of atm [38], resulting in a nonuniform tensile strain [39]. Samples with lower strain (described later) and an unstrained WS<sub>2</sub> ML were also measured for comparison. Magneto- $\mu$ -PL was performed at room temperature either in a Bitter magnet [40] up to 28.5 T or in a

superconducting magnet up to 12 T; see Supplemental Material [41], Methods. The field was perpendicular to the sample surface; see Supplemental Material [41], Note I.

*Strain dependence of energy bands and excitons.*—We performed density functional theory calculations [7,42–61] to evaluate the band structure of WS<sub>2</sub> ML under different biaxial strain values; see Fig. 1(a) and details in Supplemental Material [41], Notes I and II. The calculations were performed on planar geometries, the curvature being negligible at the atom scale due to the small height-to-radius ratio and relatively large spatial extent of the deformation (few  $\mu\text{m}$ ) of the bubbles. The CB minimum sits at *K*, where the spin-split upper (CB<sub>+</sub>) and lower (CB<sub>-</sub>) energy states are separated by 33 meV. The VB maximum is initially represented by the upper spin-split state at *K* (VB<sub>+</sub>). However, when a strain  $\varepsilon_{\text{biax}} = 2.0\%$  is reached, the VB maximum shifts to  $\Gamma$  (VB <sub>$\Gamma$</sub> ), and a crossover from a direct to an indirect band gap occurs. The exciton crossover occurs at lower strains of  $\sim 1.1\%$  due to the larger binding energy of indirect excitons [33]; see Supplemental Material [41], Note I. This transition was recently experimentally observed in WS<sub>2</sub> bubbles [37].

Figure 1(b) shows the microscope image of a typical flake with one-layer-thick bubbles. The bubbles host a similar strain distribution regardless of their size. The strain is predictable via numerical [35,39] or analytical [39] calculations and changes from uniaxial at the bubble edge to biaxial at its summit, where it reaches its maximum value [36,37,39]; see Supplemental Material [41], Note I. Since

the electronic response to strain is independent of the strain character (uniaxial or biaxial), as shown in Supplemental Material [41], Note I, and in agreement with Ref. [62], the relevant information can be embedded in an “equivalent biaxial strain”  $\varepsilon_{\text{biax}}$  defined as the average of the two in-plane strain components. The strain increases from the bubble edge toward the center, influencing the optoelectronic properties of the ML. The PL spectrum of a strain-free ML is dominated by the A exciton at 2.02 eV. The same transition is observed at the edge of the bubbles, but it is redshifted due to strain [Fig. 1(c)]. Toward the summit, a new band appears and totally dominates the spectrum at the center. This band is attributed to the indirect I exciton, features longer decay times and is less intense [37]. In small bubbles, where the spatial resolution is not sufficiently high, the A exciton dominates due to its higher recombination efficiency. Therefore, A and I excitons can be separately observed in bubbles of different dimensions.

*g factors from first-principles.*—While the direct-to-indirect exciton transition has been predicted in many theoretical works [51,62–66], a compelling analysis of the I exciton in terms of bands and symmetries and of the  $g$  factor of A and I excitons under strain is lacking. To characterize the  $g$  factor, one has to quantify the spin ( $S_z$ ) and orbital ( $L_z$ ) angular momentum of the energy bands involved in the exciton transitions. Figure 1(d) shows the schematic representation of the relevant CBs and VBs, indicating the corresponding orientation of  $S_z$  and  $L_z$ . The A exciton stems from  $\text{CB}_+$  and  $\text{VB}_+$  (with same spin), whereas the I exciton stems from  $\text{CB}_-$  (the lowest energy CB) and  $\text{VB}_\Gamma$ ; see also Supplemental Material [41], Notes III and IV. The band  $g$  factors are calculated using state-of-the-art *ab initio* techniques [53–56], which allows us to compute  $L_z$  not only at the  $K$  valleys but also at the  $\Gamma$  point. Particularly, we found  $L_z \approx 0$  for  $\text{VB}_\Gamma$  over the whole range of analyzed strain; see Supplemental Material [41], Note IV. This result agrees with previous reports on unstrained  $\text{MoSe}_2$  [54] and  $\text{WSe}_2$  [55] MLs. For the A exciton, the spin-conserving selection rules that determine the  $g$ -factor sign are readily determined by the direct transitions involving  $\text{CB}_+$  and  $\text{VB}_+$  at the  $\pm K$  valleys (with  $\sigma^\pm$  polarization) [67,68]. Conversely, to understand the magneto-PL emission of the I exciton, it is also necessary to account for the influence of phonons [69]. From a systematic analysis of the phonon-mediated selection rules using group theory [70–73], we found that different phonons with wave vector  $K$  (namely, the  $K_4$  or a pair of  $K_5$ ,  $K_6$ ) could mediate the radiative recombination between  $\text{CB}_-$  and  $\text{VB}_\Gamma$  and lead to a ZS of two oppositely circularly polarized components. Combining the symmetry analysis of the optical transitions and first-principles calculations of the orbital angular momentum, we summarize the dependence of the effective  $g$  factors of A and I excitons in Fig. 1(e), for both biaxial and uniaxial strain. Specifically,

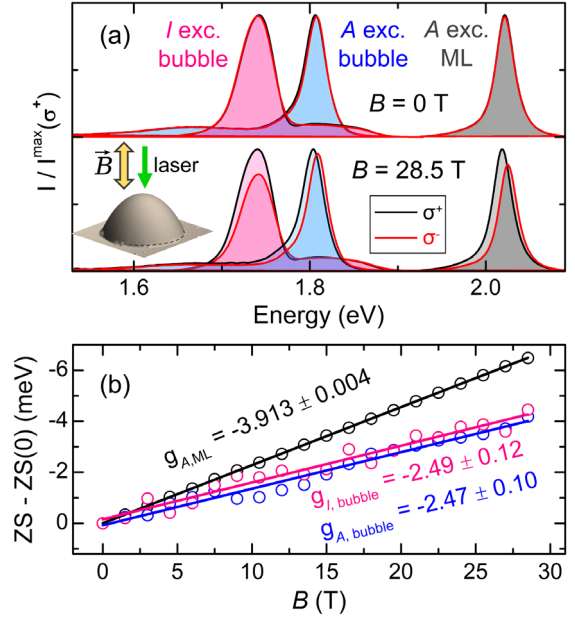


FIG. 2. (a)  $B = 0.0$  T and  $B = 28.5$  T room-temperature  $\mu$ -PL spectra filtered by circular polarization  $\sigma_\pm$ . The gray-shaded spectra refer to the A exciton of the unstrained ML. The light-blue-shaded and pink-shaded spectra refer to the A and I exciton, respectively, of two  $\text{WS}_2$  bubbles. Inset: sketch of the magneto- $\mu$ -PL experiment on a single  $\text{WS}_2$  bubble. (b) ZS vs  $B$  for the same samples. The error bars are not displayed for ease of visualization (see Supplemental Material [41], Note VI-A).

$$g_A = 2[L_z(\text{CB}_+) - L_z(\text{VB}_+)] \quad (2)$$

$$g_I = 2|L_z(\text{CB}_-) - 2|, \quad (3)$$

$L_z$  being calculated at different strain values. Our results reveal that strain slightly alters the  $g$  factors of both A and I excitons. Since the radiative emission of the indirect exciton can be mediated by different phonons, we could not determine its  $g$  factor sign and thus considered both the case of  $g_I > 0$  and  $g_I < 0$ . For details on the selection rules, see Supplemental Material [41], Note IV.

*Experimental g factors.*—To probe the  $g$  factors of strained  $\text{WS}_2$ , we measured different bubbles, where the A or I transitions could be separately observed. Figure 2(a) shows the room-temperature  $\mu$ -PL spectra at 0 T and 28.5 T recorded on an unstrained planar ML (gray-shaded) and on two different bubbles, showing A (light-blue-shaded) and I (pink-shaded) transitions. The planar ML was deposited on a  $\text{SiO}_2/\text{Si}$  substrate. While the substrate might induce some strain transfer, such strain is negligible with respect to the bubble strains. The planar ML is thus referred to as “unstrained.”

In all cases, a clear splitting between the  $\sigma^+$  and  $\sigma^-$  components is observed at 28.5 T, but the strained bubbles feature a smaller ZS than the unstrained ML.

At 0 T, no splitting is observed for the unstrained ML, whereas a small Zeeman-like splitting can be noticed for the bubbles; see also Supplemental Material [41], Notes V and VI. We speculate that strain-induced pseudogauge fields [74,75] are at the origin of this phenomenon, which will be the object of future studies.

Figure 2(b) depicts the field dependence of the ZS for the different excitons considered. Via Eq. (1), we find  $g_{A,ML} = -3.913 \pm 0.004$  for the unstrained ML; see Supplemental Material [41], Note V, where a full characterization ( $g$  factor, diamagnetic shift, degree of circular polarization) is reported. The experimental  $g$  factor agrees well with the theoretical calculations ( $-3.84$ ) for the  $A$  exciton at zero strain [Fig. 1(e)]. Our  $g$  factor is also close to those estimated in previous works [6,8,9,12,13], where, however, the measurements were performed at  $\sim 4.2$  K. This implies that temperature does not influence much the physics of  $g_{exc}$ . This agrees with recent predictions [53], showing how  $g_{exc}$  remains nearly unchanged when the band gap is modified, at variance with band  $g$  factors.

Figure 2(b) also shows the ZS obtained for the bubbles. Interestingly, we find  $g_{A,bubble} = -2.47 \pm 0.10$ , which amounts to a 40% decrease with respect to the unstrained ML. Equally interestingly,  $g_{I,bubble} = -2.49 \pm 0.12$ , remarkably close to  $g_{A,bubble}$ . We studied several other bubbles and estimated  $g_{exc}$  for  $A$ -type or  $I$ -type excitons subject to slightly different strain values, finding similar  $g$  factors, as detailed in Supplemental Material [41], Note VI. These results clearly contrast with the pure density functional theory picture given in Fig. 1(e). To understand the role of strain in determining the  $g$ -factor variation, we studied samples characterized by lower strains. In particular, in a  $WS_2$  bubble with elongated geometry we observed a redshift of 90 meV ( $\epsilon_{biax} \approx 0.7\%$ ) and in a  $WS_2$  ML deposited on a hBN bubble [76] a small strain transfer was achieved, resulting in a redshift of 7 meV ( $\epsilon_{biax} \approx 0.06\%$ ). In both cases,  $A$  exciton  $g$  factors close to  $-4$  were measured; see Supplemental Material [41], Note VI. This proves that high strains are necessary to affect  $g_{exc}$ .

It should be noticed that Ref. [19] reported on  $g$  factors between  $-2$  and  $-4$  measured at 4.2 K in some  $WSe_2$  MLs subject to small uniaxial strains (redshifts  $< 6$  meV) ( $g_{A,ML} = -4.02$  and  $-4.6$  were measured in unstrained MLs), accompanied by an exciton splitting, which was attributed to a strain-induced intervalley electron-hole exchange interaction [19]. In our case, however, neither an exciton splitting nor a  $g$ -factor variation was observed in the  $WS_2$  ML deposited on a hBN bubble [76], characterized by similar strains. We also repeated the same experiment by depositing a  $WSe_2$  ML on hBN bubbles [76], achieving a redshift of 10 meV. Again, we found no splitting and a  $g$  factor comparable to that of an unstrained ML; see Supplemental Material [41], Note VII. The discrepancy between our results and those of Ref. [19] requires further investigation, which is beyond the scope of this work.

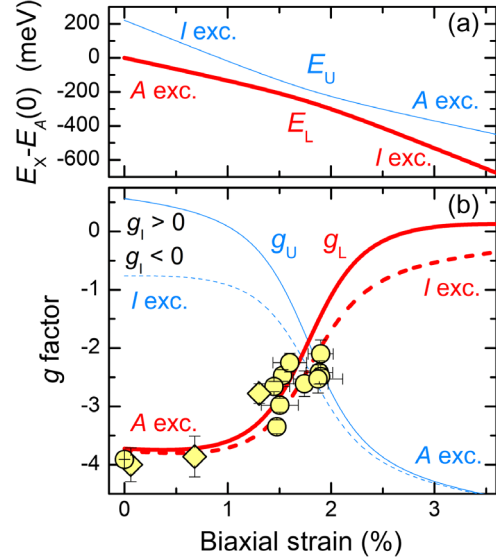


FIG. 3. (a) Energy dependence of the  $U$  and  $L$  branches vs strain for  $B = 0$  T. The hybridization parameters are  $\Delta = 35$  meV,  $E_I(0) - E_A(0) = 210$  meV,  $\Delta E_A = -128$  meV/%, and  $\Delta E_I = -246$  meV/%. (b) Calculated and experimental  $g$  factors. Circles (diamonds) refer to  $g$  factors measured in the Bitter (superconducting) magnet. Solid (dashed) lines were obtained assuming  $g_I > (<) 0$ . The hybridization parameters are  $g_A = -3.84$ ,  $\Delta g_A = -0.23$ ,  $g_I = 0.68$ , and  $\Delta g_I = -0.12$  [obtained from Fig. 1(e)].

*Exciton hybridization and  $g$ -factor renormalization.*—To interpret the experimental  $g$  factors of  $\sim -2.5$  in highly strained  $WS_2$  bubbles [Fig. 2(b)], we recall that our first-principles calculations [Fig. 1(e)] clearly establish that neither  $g_A$  nor  $g_I$  is strongly altered by strain at the orbital level. This suggests that additional mechanisms, beyond purely orbital effects, are responsible for the  $g$ -factor renormalization. Since the two exciton species become energy-resonant for increasing strain, we consider exciton hybridization. For a generic coupling between excitons, either even or odd with respect to time-reversal symmetry, the strain and magnetic field dependence of the coupled  $A$  and  $I$  excitons can be described by the upper ( $U$ ) and lower ( $L$ ) branches following these relations:

$$\begin{aligned}
 E_{U\pm}(\epsilon) &= \frac{E_+(\epsilon) \pm G_+(\epsilon)}{2} + \sqrt{\left[\frac{E_-(\epsilon) \pm G_-(\epsilon)}{2}\right]^2 + \Delta^2} \\
 E_{L\pm}(\epsilon) &= \frac{E_+(\epsilon) \pm G_+(\epsilon)}{2} - \sqrt{\left[\frac{E_-(\epsilon) \pm G_-(\epsilon)}{2}\right]^2 + \Delta^2}.
 \end{aligned}
 \tag{4}$$

Here, the subindex  $\pm$  refers to the  $\sigma^\pm$  component,  $\Delta$  is the coupling parameter encoding the exciton hybridization, and  $E_\pm$  and  $G_\pm$  are given by

$$\begin{aligned}
 E_{\pm}(\varepsilon) &= E_A(\varepsilon) \pm E_I(\varepsilon) \\
 G_{\pm}(\varepsilon) &= \frac{1}{2}\mu_B B [g_A(\varepsilon) \pm g_I(\varepsilon)], \quad (5)
 \end{aligned}$$

where  $E_{A(I)}(\varepsilon)$  and  $g_{A(I)}(\varepsilon)$  depend linearly on strain ( $E_{A(I)}(\varepsilon) = E_{A(I)}(0) + \Delta E_{A(I)}\varepsilon$  and  $g_{A(I)}(\varepsilon) = g_{A(I)}(0) + \Delta g_{A(I)}\varepsilon$ ) [see, e.g., Fig. 1(e)]. See Note VIII of the Supplemental Material [41] for the explicit form of the hybridization Hamiltonian and details.

Figure 3(a) shows the effect of exciton hybridization on the energy levels  $E_U$  and  $E_L$  (at zero magnetic field). At zero strain, the  $A$  exciton is below the  $I$  exciton. With increasing strain, the two excitons hybridize, marked by a distinct anticrossing in the energy levels. Eventually, for sufficiently large strain, the two exciton species are decoupled again and the  $I$  exciton is below the  $A$  exciton. Interestingly, this anticrossing has never been observed experimentally in a 2D system, which is different from, e.g., bulk semiconductor alloys [77]. Indeed, strain-induced exciton transitions (direct-to-indirect for MLs, indirect-to-direct for bilayers) were predicted [51,62,65,66] and observed [37,78–80] in several TMDs. Clear-cut evidence was, however, reported only at room temperature and in microscopic structures with variable strain [37,78]. In these circumstances, exciton funneling makes it difficult to establish experimentally a relationship between energy and strain [33,37,81], and the width of PL bands is comparable to the  $L/U$  separation in the hybridization region. These factors possibly prevented the observation of exciton anticrossing.

In the presence of magnetic fields, the  $g$  factors associated with the  $U$  ( $L$ ) exciton branches are given by  $g_{U(L)}(\varepsilon) = [E_{U(L)+} - E_{U(L)-}]/\mu_B B$ . Figure 3(b) compares the theoretical trends with the experimentally measured  $g$  factors. The strain corresponding to each experimental datum was deduced from the theoretical relationship between exciton energy and strain displayed in panel (a), where the experimental exciton recombination energy  $E_X$  is determined from the PL measurements; see further details in Supplemental Material, Note IX. For small strains ( $\leq 1\%$ ),  $g_L$  remains nearly unchanged. As strain increases and we enter the hybridization region,  $g_L$  increases (toward  $g_I$ ) and  $g_U$  decreases (toward  $g_A$ ). The experimental  $g$  factors nicely fall onto the calculated curves of  $g_L$ , which corresponds to the  $E_L$  branch favored in PL. Interestingly, the majority of the measured  $g$  factors lies in the strain range 1.5% to 2%, where the largest hybridization is achieved. In our analysis, we still consider the two possible signs of  $g_I$  but we emphasize that in the strong hybridization regime the  $g_I$  sign uncertainty is less pronounced. In Note VIII-B in the Supplemental Material [41] we study the behavior of  $g_U$  and  $g_L$  with different parameter sets.

The crucial ingredient for exciton hybridization is the coupling parameter  $\Delta$ . Although we introduced such coupling phenomenologically, we further elaborate on its

possible microscopic origin. Recent studies showed that pure exciton-exciton interactions are of the order of few meV [82], whereas phonon-mediated exciton-exciton interactions may reach tens of meV [83]. In Fig. 3, we found the best agreement for  $\Delta = 35$  meV, thus suggesting that phonons are mediating the exciton hybridization. Interestingly, for such phonon-mediated coupling, decreasing the temperature would decrease  $\Delta$  [83], resulting in a steeper slope of  $g_{U(L)}$  vs strain. Phenomenological approaches akin to ours have recently been used to explain hybridization signatures between dark and  $B$  ( $CB_-$ ,  $VB_-$ ) excitons [84] and between  $A$  and  $B$  excitons [85] in bilayer  $\text{MoS}_2$ . These observations call for further theoretical efforts to provide a deeper microscopic understanding of exciton hybridization mechanisms in van der Waals materials.

*Conclusions.*—We showed that strain induces a hybridization of  $k$ -direct and  $k$ -indirect excitons in mechanically deformed  $\text{WS}_2$  MLs. The hybridization—otherwise hard to unveil by the exciton energy behavior—was apparent from ZS measurements on  $\text{WS}_2$  microbubbles. Indeed, a drastic reduction of the exciton  $g$ -factor modulus was found and well reproduced by a combination of first-principles calculations and phenomenological modeling of the exciton interaction. The strain dependence of  $g_{\text{exc}}$  highlighted the pivotal role that mechanical deformations play in the encoding and reading of the valley quantum number of excitons. Our study also demonstrates that ZS measurements can be a fine tool to highlight exciton hybridization phenomena, thus providing a reference for future research in the field of 2D materials and heterostructures, where hybridization phenomena between resonant exciton species could play a fundamental role in tuning the system properties.

This work was supported by HFML-RU/NWO-I, member of the European Magnetic Field Laboratory (EMFL), and by the European Union’s Horizon 2020 research and innovation program through the ISABEL project (No. 871106). P. E. F. J., K. Ž., and J. F. acknowledge the financial support by the Deutsche Forschungsgemeinschaft (DFG, German Research Foundation) SFB 1277 (Project No. 314695032), SPP 2244 (Project No. 443416183), and the European Union Horizon 2020 Research and Innovation Program under Contract No. 881603 (Graphene Flagship). A. S. gratefully acknowledges funding from the European Union’s Horizon 2020 research and innovation program under the Marie Skłodowska-Curie grant agreement No. 844837. We acknowledge support from the National Science Centre, Poland, through Grants No. 2018/31/B/ST3/02111 (K. O.-P. and M. R. M.) and No. 2017/27/B/ST3/00205 (A. B. and T. K.). The Polish participation in the EMFL is supported by the DIR/WK/2018/07 Grant from Polish Ministry of Education and Science. T. W. acknowledges the financial support of National Science Centre, Poland within Project No. 2021/41/N/ST3/04516 and the

support of the Center for Information Services and HPC (ZIH) at TU Dresden for computational resources. A. Č. acknowledges funding from the Brazilian Research Council (CNPq), under the PQ and UNIVERSAL programs, and from the Research Foundation—FLANDERS (FWO).

\*Corresponding author.

elena.blundo@uniroma1.it

†Corresponding author.

fariajunior.pe@gmail.com

‡Corresponding author.

antonio.polimeni@uniroma1.it

- [1] G. Wang, A. Chernikov, M. M. Glazov, T. F. Heinz, X. Marie, T. Amand, and B. Urbaszek, *Rev. Mod. Phys.* **90**, 021001 (2018).
- [2] M. Koperski, M. R. Molas, A. Arora, K. Nogajewski, A. O. Slobodeniuk, C. Faugeras, and M. Potemski, *Nanophotonics* **6**, 1289 (2017).
- [3] Y. Liu, Y. Gao, S. Zhang, J. He, J. Yu, and Z. Liu, *Nano Res.* **12**, 2695 (2019).
- [4] G. Aivazian, Z. Gong, A. M. Jones, R.-L. Chu, J. Yan, D. G. Mandrus, C. Zhang, D. Cobden, W. Yao, and X. Xu, *Nat. Phys.* **11**, 148 (2015).
- [5] D. MacNeill, C. Heikes, K. F. Mak, Z. Anderson, A. Kormányos, V. Zolyomi, J. Park, and D. C. Ralph, *Phys. Rev. Lett.* **114**, 037401 (2015).
- [6] J. Zipfel, J. Holler, A. A. Mitioglu, M. V. Ballottin, P. Nagler, A. V. Stier, T. Taniguchi, K. Watanabe, S. A. Crooker, P. C. M. Christianen *et al.*, *Phys. Rev. B* **98**, 075438 (2018).
- [7] M. Zinkiewicz, T. Woźniak, T. Kazimierczuk, P. Kapuscinski, K. Oreszczuk, M. Grzeszczyk, M. Bartoś, K. Nogajewski, K. Watanabe, T. Taniguchi *et al.*, *Nano Lett.* **21**, 2519 (2021).
- [8] G. Plechinger, P. Nagler, A. Arora, A. Granados del Águila, M. V. Ballottin, T. Frank, P. Steinleitner, M. Gmitra, J. Fabian, P. C. Christianen *et al.*, *Nano Lett.* **16**, 7899 (2016).
- [9] A. V. Stier, K. M. McCreary, B. T. Jonker, J. Kono, and S. A. Crooker, *Nat. Commun.* **7**, 10643 (2016).
- [10] R. Schmidt, A. Arora, G. Plechinger, P. Nagler, A. G. del Águila, M. V. Ballottin, P. C. M. Christianen, S. M. de Vasconcellos, C. Schüller, T. Korn *et al.*, *Phys. Rev. Lett.* **117**, 077402 (2016).
- [11] J. Kuhnert, A. Rahimi-Iman, and W. Heimbrod, *J. Phys. Condens. Matter* **29**, 08LT02 (2017).
- [12] M. Koperski, M. R. Molas, A. Arora, K. Nogajewski, M. Bartos, J. Wyzula, D. Vaclavkova, P. Kossacki, and M. Potemski, *2D Mater.* **6**, 015001 (2018).
- [13] M. Goryca, J. Li, A. V. Stier, T. Taniguchi, K. Watanabe, E. Courtade, S. Shree, C. Robert, B. Urbaszek, X. Marie *et al.*, *Nat. Commun.* **10**, 4172 (2019).
- [14] A. A. Mitioglu, P. Plochocka, A. G. del Águila, P. C. M. Christianen, G. Deligeorgis, S. Anghel, L. Kulyuk, and D. K. Maude, *Nano Lett.* **15**, 4387 (2015).
- [15] G. Wang, L. Bouet, M. M. Glazov, T. Amand, E. L. Ivchenko, E. Palleau, X. Marie, and B. Urbaszek, *2D Mater.* **2**, 034002 (2015).
- [16] A. Srivastava, M. Sidler, A. Allain, D. Lembke, A. Kis, and A. Imamoglu, *Nat. Phys.* **11**, 141 (2015).
- [17] A. V. Stier, N. P. Wilson, G. Clark, X. Xu, and S. A. Crooker, *Nano Lett.* **16**, 7054 (2016).
- [18] A. V. Stier, N. P. Wilson, K. A. Velizhanin, J. Kono, X. Xu, and S. A. Crooker, *Phys. Rev. Lett.* **120**, 057405 (2018).
- [19] A. Mitioglu, J. Buhot, M. V. Ballottin, S. Anghel, K. Sushkevich, L. Kulyuk, and P. C. M. Christianen, *Phys. Rev. B* **98**, 235429 (2018).
- [20] S.-Y. Chen, Z. Lu, T. Goldstein, J. Tong, A. Chaves, J. Kunstmann, L. S. R. Cavalcante, T. Woźniak, G. Seifert, D. R. Reichman *et al.*, *Nano Lett.* **19**, 2464 (2019).
- [21] M. R. Molas, A. O. Slobodeniuk, T. Kazimierczuk, K. Nogajewski, M. Bartos, P. Kapuściński, K. Oreszczuk, K. Watanabe, T. Taniguchi, C. Faugeras *et al.*, *Phys. Rev. Lett.* **123**, 096803 (2019).
- [22] C. Robert, B. Han, P. Kapuscinski, A. Delhomme, C. Faugeras, T. Amand, M. Molas, M. Bartos, K. Watanabe, T. Taniguchi *et al.*, *Nat. Commun.* **11**, 4037 (2020).
- [23] P. Nagler, M. V. Ballottin, A. A. Mitioglu, F. Mooshammer, N. Paradiso, C. Strunk, R. Huber, A. Chernikov, P. C. M. Christianen, C. Schüller *et al.*, *Nat. Commun.* **8**, 1551 (2017).
- [24] A. Ciarrocchi, D. Unuchek, A. Avsar, K. Watanabe, T. Taniguchi, and A. Kis, *Nat. Photonics* **13**, 131 (2019).
- [25] T. Wang, S. Miao, Z. Li, Y. Meng, Z. Lu, Z. Lian, M. Blei, T. Taniguchi, K. Watanabe, S. Tongay *et al.*, *Nano Lett.* **20**, 694 (2020).
- [26] A. Surrente, Ł. Kłopotowski, N. Zhang, M. Baranowski, A. A. Mitioglu, M. V. Ballottin, P. C. Christianen, D. Dumcenco, Y.-C. Kung, D. K. Maude *et al.*, *Nano Lett.* **18**, 3994 (2018).
- [27] K. L. Seyler, P. Rivera, H. Yu, N. P. Wilson, E. L. Ray, D. G. Mandrus, J. Yan, W. Yao, and X. Xu, *Nature (London)* **567**, 66 (2019).
- [28] H. Baek, M. Brotons-Gisbert, Z. X. Koong, A. Campbell, M. Rambach, K. Watanabe, T. Taniguchi, and B. D. Gerardot, *Sci. Adv.* **6**, eaba8526 (2020).
- [29] Y. Sun, S. E. Thompson, and T. Nishida, *J. Appl. Phys.* **101**, 104503 (2007).
- [30] M. L. Lee, E. A. Fitzgerald, M. T. Bulsara, M. T. Currie, and A. Lochtefeld, *J. Appl. Phys.* **97**, 011101 (2005).
- [31] G. Pettinari, A. Polimeni, F. Masia, R. Trotta, M. Felici, M. Capizzi, T. Niebling, W. Stolz, and P. J. Klar, *Phys. Rev. Lett.* **98**, 146402 (2007).
- [32] J. Liu, X. Sun, R. Camacho-Aguilera, L. C. Kimerling, and J. Michel, *Opt. Lett.* **35**, 679 (2010).
- [33] E. Blundo, E. Cappelluti, M. Felici, G. Pettinari, and A. Polimeni, *Appl. Phys. Rev.* **8**, 021318 (2021).
- [34] C. Di Giorgio, E. Blundo, G. Pettinari, M. Felici, F. Bobba, and A. Polimeni, *Adv. Mater. Interfaces* **9**, 2102220 (2022).
- [35] D. Tedeschi, E. Blundo, M. Felici, G. Pettinari, B. Liu, T. Yildirim, E. Petroni, C. Zhang, Y. Zhu, S. Sennato *et al.*, *Adv. Mater.* **31**, 1903795 (2019).
- [36] E. Blundo, C. Di Giorgio, G. Pettinari, T. Yildirim, M. Felici, Y. Lu, F. Bobba, and A. Polimeni, *Adv. Mater. Interfaces* **7**, 2000621 (2020).
- [37] E. Blundo, M. Felici, T. Yildirim, G. Pettinari, D. Tedeschi, A. Miriametro, B. Liu, W. Ma, Y. Lu, and A. Polimeni, *Phys. Rev. Research* **2**, 012024(R) (2020).

- [38] C. Di Giorgio, E. Blundo, G. Pettinari, M. Felici, Y. Lu, A. M. Cucolo, A. Polimeni, and F. Bobba, *Adv. Mater. Interfaces* **7**, 2001024 (2020).
- [39] E. Blundo, T. Yildirim, G. Pettinari, and A. Polimeni, *Phys. Rev. Lett.* **127**, 046101 (2021).
- [40] D. Tedeschi, M. De Luca, P. E. Faria Junior, A. G. del Águila, Q. Gao, H. H. Tan, B. Scharf, P. C. M. Christianen, C. Jagadish, J. Fabian *et al.* *Phys. Rev. B* **99**, 161204(R) (2019).
- [41] See Supplemental Material at <http://link.aps.org/supplemental/10.1103/PhysRevLett.129.067402> for the Methods Section, and notes on (i) magneto- $\mu$ -PL measurements on WS<sub>2</sub> bubbles; (ii) first-principles calculations; (iii) transition energies as function of strain; (iv) identifying the indirect exciton  $g$  factor; (v) strain-free monolayer analysis:  $g$  factor, diamagnetic shift, and degree of circular polarization; (vi)  $g$  factors of direct and indirect excitons in strained WS<sub>2</sub> monolayers; (vii) WSe<sub>2</sub> monolayer analysis of the  $g$  factor at low and null strain; (viii) hybridization of direct and indirect excitons; (ix) strain evaluation in WS<sub>2</sub> bubbles.
- [42] P. Giannozzi, S. Baroni, N. Bonini, M. Calandra, R. Car, C. Cavazzoni, D. Ceresoli, G. L. Chiarotti, M. Cococcioni, I. Dabo *et al.*, *J. Phys. Condens. Matter* **21**, 395502 (2009).
- [43] G. Kresse and D. Joubert, *Phys. Rev. B* **59**, 1758 (1999).
- [44] J. P. Perdew, A. Ruzsinszky, G. I. Csonka, O. A. Vydrov, G. E. Scuseria, L. A. Constantin, X. Zhou, and K. Burke, *Phys. Rev. Lett.* **100**, 136406 (2008).
- [45] P. Blaha, K. Schwarz, F. Tran, R. Laskowski, G. K. Madsen, and L. D. Marks, *J. Chem. Phys.* **152**, 074101 (2020).
- [46] D. J. Singh and L. Nordstrom, *Planewaves, Pseudopotentials, and the LAPW Method* (Springer Science & Business Media, New York, 2006).
- [47] M. Rohlfing and S. G. Louie, *Phys. Rev. B* **62**, 4927 (2000).
- [48] N. S. Rytova, *Moscow Univ. Phys. Bull.* **3**, 18 (1967), <http://vnu.phys.msu.ru/abstract/1967/3/1967-3-030/>.
- [49] L. Keldysh, *Sov. J. Exp. Theor. Phys. Lett.* **29**, 658 (1979), [http://jetpletters.ru/ps/1458/article\\_22207.shtml](http://jetpletters.ru/ps/1458/article_22207.shtml).
- [50] P. Cudazzo, I. V. Tokatly, and A. Rubio, *Phys. Rev. B* **84**, 085406 (2011).
- [51] K. Zollner, P. E. Faria Junior, and J. Fabian, *Phys. Rev. B* **100**, 195126 (2019).
- [52] A. Kormányos, G. Burkard, M. Gmitra, J. Fabian, V. Zólyomi, N. D. Drummond, and V. Fal'ko, *2D Mater.* **2**, 022001 (2015).
- [53] T. Woźniak, P. E. Faria Junior, G. Seifert, A. Chaves, and J. Kunstmann, *Phys. Rev. B* **101**, 235408 (2020).
- [54] T. Deilmann, P. Krüger, and M. Rohlfing, *Phys. Rev. Lett.* **124**, 226402 (2020).
- [55] J. Förste, N. V. Tepliakov, S. Y. Kruchinin, J. Lindlau, V. Funk, M. Förg, K. Watanabe, T. Taniguchi, A. S. Baimuratov, and A. Högele, *Nat. Commun.* **11**, 4539 (2020).
- [56] F. Xuan and S. Y. Quek, *Phys. Rev. Research* **2**, 033256 (2020).
- [57] C. Robert, H. Dery, L. Ren, D. Van Tuan, E. Courtade, M. Yang, B. Urbaszek, D. Lagarde, K. Watanabe, T. Taniguchi *et al.*, *Phys. Rev. Lett.* **126**, 067403 (2021).
- [58] T. C. Berkelbach, M. S. Hybertsen, and D. R. Reichman, *Phys. Rev. B* **88**, 045318 (2013).
- [59] P. E. Faria Junior, M. Kurpas, M. Gmitra, and J. Fabian, *Phys. Rev. B* **100**, 115203 (2019).
- [60] K. Zollner, P. E. Faria Junior, and J. Fabian, *Phys. Rev. B* **100**, 085128 (2019).
- [61] F. Dirnberger, J. D. Ziegler, P. E. Faria Junior, R. Bushati, T. Taniguchi, K. Watanabe, J. Fabian, D. Bougeard, A. Chernikov, and V. M. Menon, *Sci. Adv.* **7**, eabj3066 (2021).
- [62] P. Johari and V. B. Shenoy, *ACS Nano* **6**, 5449 (2012).
- [63] M. Ghorbani-Asl, S. Borini, A. Kuc, and T. Heine, *Phys. Rev. B* **87**, 235434 (2013).
- [64] H. Shi, H. Pan, Y.-W. Zhang, and B. I. Yakobson, *Phys. Rev. B* **87**, 155304 (2013).
- [65] C.-H. Chang, X. Fan, S.-H. Lin, and J.-L. Kuo, *Phys. Rev. B* **88**, 195420 (2013).
- [66] L. Ortenzi, L. Pietronero, and E. Cappelluti, *Phys. Rev. B* **98**, 195313 (2018).
- [67] D. Xiao, G.-B. Liu, W. Feng, X. Xu, and W. Yao, *Phys. Rev. Lett.* **108**, 196802 (2012).
- [68] K. F. Mak, K. He, J. Shan, and T. F. Heinz, *Nat. Nanotechnol.* **7**, 494 (2012).
- [69] T. Inui, Y. Tanabe, and Y. Onodera, *Group Theory and its Applications in Physics* (Springer Science & Business Media, Berlin, 2012), Vol. 78.
- [70] J. Ribeiro-Soares, R. M. Almeida, E. B. Barros, P. T. Araujo, M. S. Dresselhaus, L. G. Cançado, and A. Jorio, *Phys. Rev. B* **90**, 115438 (2014).
- [71] B. Peng, H. Zhang, H. Shao, Y. Xu, R. Zhang, and H. Zhu, *J. Mater. Chem. C* **4**, 3592 (2016).
- [72] G. F. Koster, J. O. Dimmock, R. G. Wheeler, and H. Statz, *Properties of the Thirty-Two Point Groups* (MIT Press, Cambridge, MA, 1963), Vol. 24.
- [73] M. S. Dresselhaus, G. Dresselhaus, and A. Jorio, *Group Theory: Application to the Physics of Condensed Matter* (Springer Science & Business Media, Berlin, 2007).
- [74] M. Vozmediano, M. Katsnelson, and F. Guinea, *Phys. Rep.* **496**, 109 (2010).
- [75] H. Rostami, R. Roldán, E. Cappelluti, R. Asgari, and F. Guinea, *Phys. Rev. B* **92**, 195402 (2015).
- [76] E. Blundo, A. Surrente, D. Spirito, G. Pettinari, T. Yildirim, C. A. Chavarin, L. Baldassarre, M. Felici, and A. Polimeni, *Nano Lett.* **22**, 1525 (2022).
- [77] M. Capizzi, S. Modesti, F. Martelli, and A. Frova, *Solid State Commun.* **39**, 333 (1981).
- [78] J. Chaste, A. Missaoui, S. Huang, H. Henck, Z. B. Aziza, L. Ferlazzo, C. Naylor, A. Balan, J. Alan T. Charlie Johnson, R. Braive *et al.*, *ACS Nano* **12**, 3235 (2018).
- [79] Y. Wang, C. Cong, W. Yang, J. Shang, N. Peimyoo, Y. Chen, J. Kang, J. Wang, W. Huang, and T. Yu, *Nano Res.* **8**, 2562 (2015).
- [80] S. B. Desai, G. Seol, J. S. Kang, H. Fang, C. Battaglia, R. Kapadia, J. W. Ager, J. Guo, and A. Javey, *Nano Lett.* **14**, 4592 (2014).
- [81] A. Castellanos-Gomez, R. Roldán, E. Cappelluti, M. Buscema, F. Guinea, H. S. J. van der Zant, and G. A. Steele, *Nano Lett.* **13**, 5361 (2013).
- [82] D. Erckensten, S. Brem, and E. Malic, *Phys. Rev. B* **103**, 045426 (2021).
- [83] M. Selig, G. Berghäuser, A. Raja, P. Nagler, C. Schüller, T. F. Heinz, T. Korn, A. Chernikov, E. Malic, and A. Knorr, *Nat. Commun.* **7**, 13279 (2016).
- [84] T. Deilmann and K. S. Thygesen, *Nano Lett.* **18**, 2984 (2018).
- [85] E. Lorchat, M. Selig, F. Katsch, K. Yumigeta, S. Tongay, A. Knorr, C. Schneider, and S. Höfling, *Phys. Rev. Lett.* **126**, 037401 (2021).